Investigation of eutectic island formation in SX superalloys

Warnken, N.; Ma, D.; Mathes, M.; Steinbach, I.

DOI:
10.1016/j.msea.2005.09.067

Investigation of eutectic island formation in SX-Superalloys

N. Warnken *, D. Ma , M. Mathes , I. Steinbach

ACCESS e.V., Intzestr. 5, D-52075 Aachen, Germany

Abstract

We investigated whether the nucleation of the eutectic islands in superalloy solidification occurs in the interdendritic bulk liquid or at the dendrite - melt interface. Directionally solidified samples of CMSX-4 and a model superalloy have been analysed by means of light and electron microscopy and by EBSD measurements. For some samples the solid - melt interface has been revealed by an artificial bubble technique. Additionally thermodynamic calculations on phase formation and nucleation work as well as phase-field simulations have been performed, using ThermoCalc and MICRESS. The results indicate a kind of epitaxial nucleation mechanism at the solid-liquid interface of the primary γ dendrites.

Key words: superalloy, eutectic island, nucleation, microstructure simulation, EBSD

PACS:

* Corresponding Author. Tel. +49 241 8098029 Fax +49 241 38578
Email address: n.warnken@access.rwth-aachen.de (N. Warnken).

1 Introduction

Superalloys are class of alloys widely used for high temperature applications. Due to the absence of grain boundaries single crystalline (SX) superalloys show great improvement over multigrained directional or equiaxed ones. SX Superalloys commonly are based on Ni with major additions of Al, Cr, Ta, Ti and W among others. The microstructure consists basically of the γ matrix and γ' precipitates. The superior high temperature properties are achieved due to the formation of large fractions (app. 70%) of γ' [1]. Upon cooling the γ' phase precipitates coherently from the γ matrix. Both phases have similar crystal structures. The γ phase has a disordered fcc structure ($A1$). The γ' phases is a $L1_2$ structure. The lattice misfit for both phases is usually in the order of $\delta = 0.2\%$, but depends on the alloy composition. During solidification the alloying elements segregate heavily between the phases. The γ phase is the primary phase in solidification. Typically the γ' forming elements, such as Al, Ti and Ta, enrich in the melt, while the elements W and Cr are enriched in the γ dendrites. Thus towards the end of solidification γ' starts to form large precipitates in the interdendritic regions [2]. This is commonly entitled as the $\gamma - \gamma'$, or simply as eutectic islands, although it has been established that the phase transformation is a peritectic one [4,5]. The interdendritic γ' precipitates are undesired for the final microstructure of the cast part. Thus a solution and aging heat treatment is done after the solidification, the aim of which is to reduce the amount of interdendritic precipitates and reduce the microsegregation [3].

The aim of the presented work is to investigate the mechanism of the interdendritic γ' formation. Four possible nucleation sites for γ' are taken into account in our investigation. These are $liquid$ and γ bulk phases and the $liquid - \gamma$ interface, where γ' might nucleate either on the $liquid$ or γ side. In this work strong evidence is pre-

sented that γ' nucleates from the existing γ. Nuclei close or directly at the interface have the chance to grow into the melt. The subsequent growth into the melt will be faster, due to the fast transport of solute, than the growth into the γ phase. As γ' precipitates coherently from γ, the crystal orientation is transfered from the parent phase to the new crystal. In order to evaluate the proposed mechanism, orientation relationships between the precipitates and the dendrites are investigated. The mechanism is further examined with the aid of thermodynamic calculations employing the CALPHAD method, calculation of nucleation barrier and microstructure simulations.

2 Materials and experimental procedures

Two different alloys have been used for the analysis of the interdendritic phases, CMSX-4 and a model alloy, the composition of the alloys is given in Table 1. Cylindrical samples of $8mm$ in diameter where produced in an investment casting cluster of 8 samples, directionally solidified in a Bridgman furnace with a gradient of $4K/mm$ and a withdrawal speed of $3mm/min$. In order to reveal the morphology of the growing phases an artificial bubble technique was used on some of the samples. This was achieved by inserting a small ceramic part with the shape of reverted cups into the wax pattern before the ceramic shell fabrication. After dewaxing and firing the reverted cup remains in the cavity. After the casting process the 'reverted cup' is filled with melt. During the solidification the dendrites grow into the 'reverted cup' while the volume shrinkage due to the solidification will create an underpressure in the 'reverted cup'. As feeding of melt is hindered, eventually an artificial bubble forms. The melt is sucked out and the dendrites appear from the liquid. After cutting the sample carefully the dendrites were investigated

by Scanning Electron Microscopy. Fig. 1 shows the microstructure of a CMSX-4 sample revealed by this technique. The dendrites can clearly be identified. In the interdendritic regions the spherical precipitates are attached to the dendrite arms, EDX analysis has show that these are γ'. From the image it can not be deduced whether the precipitates have formed in bulk liquid and settled when the liquid was removed or nucleated at the dendrite liquid interface. This will subject to further examination in the following sections.

Samples were taken from the solidified material, polished and carefully etched with $CuCl_2$. The microstructure was investigated by means of optical and scanning electron microscopy. Additionally the orientation and phase of the crystals in the microstructure was determined using EBSD mappings. For the EBSD measurement the γ, γ' and β phases were taken into account. The phase is detected by comparing the line densities in the Kikuchi pattern, representing the lattice constants of the sample, with a predefined set of possible phases. Orientation is measured by detecting and evaluating the bands of the pattern of the tilted sample. Several mappings were done on both alloys. Fig. 2 shows an example of an interdendritic microstructure. The typical rosette like primary γ' precipitates can be observed, surrounded by secondary γ' which has precipitated from the γ bulk upon further cooling. EB SD mappings where done over parts of the dendrites and interdendritic region. The EBSD mappings showed the presence of γ, γ', no evidence for the appearance of the β phase was found. The arrangement of phases cannot clearly be identified, as the lattices of γ and γ' are very similar the two phases are unlikely to be clearly separated by EBSD measurements. Nevertheless, on grain boundaries even slight deviations between the orientations of grains could be measured. Primary γ' precipitates always showed the same crystallographic orientation as the surrounding dendrites. Thus it can be concluded that the crystal lattice of the dendrite and of the

precipitate have the same orientation.

3 Thermodynamic calculations

Thermodynamic calculations were done to investigate the sequence of phaseformation during solidification and to calculate the driving force for the nucleation of γ' in the model alloy. The ThermoCalc package and a thermodynamic database, which was especially created for this model alloy by project partners [6], were used for the calculations. Starting from the alloy composition a Scheil simulation was performed in order to calculate the temperature and the liquid composition at which the formation of the γ' phase starts. Using the database it was found that a Tungsten rich BCC phase forms as the second solid phase. As no evidence for the formation of major quantities of this phase were found in the microstructures, this phase was rejected for the remaining calculations. Then γ' forms at $1572.17K$, the corresponding liquid composition is given in Table 1 labeled as comp. A. This point corresponds to the situation where γ dendrites have formed and only a small amount of $liquid$ is left in the interdendritic region. The composition of the γ matrix at the phase boundary is given the corresponding equilibrium γ composition, labeled as comp. B in Table 1. In the following composition A in the liquid and composition B in the solid will be treated separately to investigate the question where γ' can form upon further cooling.

Fig. 3 shows superpositions of the lever-rule calculations for the compositions A and B. The remaining liquid (comp. A, solid line) starts to from γ and γ' below $1572.17K$. At the end of the solidification ($1509.25K$) app. 64% γ' has formed. The result of the lever rule calculation for this composition B is given in Fig. 3 by the dashed lines. Here the solidification is finished at $1572.17K$, and below this

temperature we see transformation of γ to γ' with a slightly less slope than in case A.

From these calculation it can be concluded that γ' can form in the interdendritic region from either the liquid bulk or the γ dendrites. In order to find out which of the possible for nucleation sites are favoured, the driving force for the formation of γ' for the nucleation sites are calculated.

4 Nucleation

The thermodynamic calculations show that it is possible to form γ' from the melt or from the γ phase, so both phases are possible parent phases for the nucleation of γ'. In order to estimate which is the favoured nucleation site, the work to form a critical nucleus is calculated for four different nucleation sites. These are the bulk $liquid$, bulk γ and the $\gamma - liquid$ interface, where γ' might nucleate either on the $liquid$ or the γ side. In the case of nucleation from the bulk is simply the nucleation of one phase from another, while at the interface three phases are involved.

According to the classical nucleation theory as it is given in standard text books [7], the work ΔG_0 necessary to form a critical radius is calculated by:

$$\Delta G_0 = \frac{16}{3}\pi\frac{\sigma^3}{\Delta g^2} \tag{1}$$

where σ is the interfacial energy and Δg the driving force for the formation of the new phase. The driving force can be calculated from the Gibbs-free-energy diagram by a parallel tangent construction, where Δg corresponds to the distance between the two parallel tangents [8].

As single crystal superalloys are highly pure alloys, a very low concentration of heterogeneous nucleation sites in the liquid bulk can be assumed. For the nucleation of γ' in γ homogeneous nucleation is widely accepted. For nucleation at the interface heterogeneous nucleation has to be considered. The work to form a critical nucleus ΔG_{het} is therefore calculated:

$$\Delta G_{het} = f * \Delta G_0 \tag{2}$$

where f is calculated from the wetting angle Θ:

$$f = \frac{1}{4}(2 + cos(\Theta))(1 - cos(\Theta))^2 \tag{3}$$

As the interfacial energy of the $\gamma - \gamma'$ interface is by a factor of 10 smaller than the $solid - liquid$ interfacial energies, the $cosine$ of the wetting angle is around 0.5 and f becomes $f = 0.156$, for nucleation on the $liquid$ side of the interface. If γ' forms on the γ side, f becomes close to unity, so the critical work is almost the same as for homogeneous nucleation.

As the formation of γ' from γ is the nucleation of a coherent phase in the solid state, the effect of the strain energy must be accounted for. In this case total driving force in equation (1) for nucleation becomes:

$$\Delta g_{total} = \Delta g - \Delta g_{strain} \tag{4}$$

Where Δg_{total} replaces Δg in eq (1). Thus the strain energy Δg_{strain} lowers the effective driving force. In their analysis of nucleation in a Ni-Al-Cr alloy [9] have estimated the strain energy from the shear modulus of pure Nickel ($\mu^{Ni}_{shear} = 1.2 * 10^{11} Nm^{-2}$) and the lattice misfit:

$$\Delta g_{strain} \approx 3.8 \mu_{shear} \delta^2 \tag{5}$$

A lattice misfit of $\delta = 0.2\%$ is used for the analysis here. In alloys the matrix phase might have a higher shear modulus, due to the presence of solution strengthening elements. Then this effect is more pronounced.

The driving force is calculated as a function of temperature using ThermoCalc and the same database as in the previous section. Calculations were done for the composition A and B for nucleation in the $liquid$, resp. γ bulk and for composition A for interfacial nucleation.

The work to form a critical nucleus was calculated using $\sigma_{\gamma'-liq} = 300.0 mJ/m^2$ and $\sigma_{\gamma'-\gamma} = 10.0 mJ/m^2$ for the corresponding interfacial energies.

The results are plotted as a function of temperature in Fig. 4, on a semilogarithmic scale. In the case of γ' nucleating from the $liquid$ bulk a higher liquidus temperature is found ($\sim 1594.0K$), thus the displayed curve goes up to higher temperatures.

In any case the values decreases by orders of magnitude for undercoolings $\Delta T = 4K$, compared to values of marginal undercooling. The effect of the strain energy on the case of nucleation from the γ phase can clearly be seen in a shift of the curve to lower temperatures, the driving force in the temperature range between $1571.0K$ and $1572.1K$ is fully compensated by the strain energy. This effect is expected to be more pronounced for higher shear moduli. The critical work for nucleation from the $liquid$ is two or three orders of magnitude larger than for nucleation from the γ phase, even for high undercoolings. This is also the case for heterogeneous nucleation from the melt at the interface.

For a given undercooling it is found from the graphs that the nucleation of γ' from γ at the $\gamma - liquid$ phase boundary shows the lowest nucleation barrier. This is consistent to conclusions from the EBSD measurements.

5 Simulation of microstructureformation

So far it was found that γ' is most likely to nucleate from the existing γ at the existing $\gamma - liquid$ interface. So the question remains whether and in which morphology γ' precipitates will grow under these condition. This was examined be simulating the microstructure formation.

The multiphase multicomponent phase-field code MICRESS was used to simulate the microstructure formation in the interdendritic region of a solidifying superalloy dendrite. In order to account for solute transport, a multicomponent diffusion solver is coupled to the phase field solver. In order to calculate the driving force of the phase transformation and the partitioning of the alloying elements, a coupling to thermodynamic calculation via the TQ interface of ThermoCalc is used. A detailed description of the phase-field model can be found in [10,11].

The simulations were done on a regular grid with a grid spacing of $\Delta x = 0.2\mu m$ and 75x100 grid points. The same interfacial energies and thermodynamic database were used as in the previous section. The simulation started at the entry to the γ' formation in the Scheil simulation, accordingly the liquid composition was set as given in Table 1 for composition A and the temperature to $1572K$. Initially the γ phase is the only present solid phase. Nucleation of γ' was enabled in the interface and in the γ matrix, in both cases the γ phase was the matrix phase. New nuclei were set when an critical undercooling of $\Delta T = 11.0K$ for nucleation in the bulk and $\Delta T = 7.2K$ for nucleation at the interface, is reached. As stresses and strains are not calculated, the effect of the strain energy on the nucleation is taking into account implicitly in the critical nucleation undercooling. The diffusion coefficient in the liquid was set to $D = 3.1\,10^{-9} m^2/s$, which was estimated for the model

alloy from the critical G/v criteria for the breakup of a planar front. For simplicity only the diagonal terms of the diffusion matrix for solid state diffusion in the γ phase were taken into account. These were calculated with dictra and the mobility database from [12]. Only very little data about diffusion in the γ' phase can be found, but a lower diffusion rate in γ' can be expected. So the diffusion coefficients in the γ' phase were set one order of magnitude lower than in γ. Due to the much faster diffusion in the melt and the short simulated time, it can be expected that solid state diffusion plays only a very small role in the simulation.

Results of the microstructure simulation are shown in Fig. 5. The images show the tungsten concentration mapping at different times of the simulation. The phases can be distinguised by their tungsten concentration, γ shows the highest tungsten concentration (white region), while γ' shows the lowest (black region) and $liquid$ lies somewhere in between (grey region). Initially only γ and $liquid$ exists. After $17.355s$ the amount of γ has increased and γ' nucleates at the interface. After $17.500s$ the γ' precipitate has grown dramatically. The main growth has occurred into the liquid bulk, while almost no growth into the γ bulk occurs, but it can be noticed that the amount of γ has reduced significantly, in the regions around the γ' precipitate grooves in the $\gamma - liquid$ interface can be observerd where the γ phase has dissolved, exhibiting a typical microstructure of a peritectic transformation. Because the diffusion in the liquid phase is much faster than in the solid phases, the melt acts as a short cut for the solute transport. The γ' phase shows a spherical morphology. Finally upon further cooling ($24.000s$) γ and γ' grow from the melt. The precipitation of secondary γ' in the γ bulk has not started yet at this point. From the microstructure simulations three regimes of γ' formation can be found. After nucleation γ' growth is very rapid, the precipitate exhibits a spherical morphology. The growth slows down when a certain amount of γ' has formed. In the

following period not much phasetrans formation is observed, but the precipitates maintain the spherical morphology, the system equilibrates. In the microstructure revealed (Fig. 1), the γ' precipitates are in one of these two states and thus show a spherical morphology. After some time γ and γ' start to grow at a moderate rate. The morphology of the γ' precipitates becomes rather elliptical. This complies to what is seen usually in the micrographs, like in Fig. 2.

6 Summary and Conclusion

The formation of interdendritic γ' in single crystal superalloys was investigate by microstructural analysis and computational methods. Results indicate a spherical growth of the precipitates into the melt while the crystal orientation of the precipitates and the primary phase are the same. By thermodynamical calculations it was shown that γ' precipitates from γ in the interdendritic regions, while the nucleation barrier is the lowest for the nucleation of γ' from the solid γ matrix at the $\gamma - liquid$ interface. For the assumption of a moderate undercooling, direct microstructure simulation showed that spherical precipitated will form, which change their morphology upon further solidification.

Although it is not possible to estimate from the presented results, which is the correct undercooling for the nucleation, strong evidence for the nucleation of γ' from γ at the $\gamma - liquid$ interface is found.

7 Acknowledgement

The authors gratefully acknowledge the financial support of the Deutsche Forschungs Gemeinschaft (DFG) within the collaborative research center 'integral materials modeling', SFB 370.

References

[1] C. T. Sims, N. S. Stoloff, W. C. Hagel (Eds.), Superalloys II, John Wiley & Sons, New York, 1987

[2] M. Durand-Charre, The Microstructure of Superalloys, Gordon and Breach Science Publishers, Amsterdam, 1997

[3] B.C. Wilson, J. A. Hickman, G.E. Fuchs, JOM 55 (2003) 35-40

[4] K. Hilpert, D. Kobertz, V. Venugopal, M. Miller, H. Gerads, F. J. Bremer, H. Nickel, Z. Naturforsch. 42A (1987) 1327-1331

[5] J.H. Lee, J.D. Verhoeven, Journal of Crystal Growth 144 (1994) 353-366

[6] Prof. Neuschütz, Lehrstuhl fuer Theorerische Huettenkunde (LTH), RWTH-Aachen

[7] G. Gottstein, Physikalische Grundlagen der Materialkunde, Springer Verlag Berlin (1998)

[8] M. Hillert, Phase Equilibria Phase Diagrams and Phase Transformations, Cambridge University Press, Cambridge, UK, 1998

[9] C. Schmuck, P. Caron, A. Hauet, D. Blavette, Philosophical Magazine A 76 (1997) 527-542

[10] I. Steinbach, F. Pezolla, B. Nestler, M. Sesselberg, R. Prieler, G. J. Schmitz, J. L. L. Rezende, Physica D 94 (1996) 135-147

[11] J. Tiaden, B. Nestler, H. J. Diepers, I. Steinbach, Physica D 115 (1998) 73-86

[12] C. E. Campbel, W. J. Boettinger, U. R. Kattner, Acta Mater. 50 (2002) 775

Table 1

Composition of the investigated alloys in at%.

	Al	Co	Cr	Re	Ta	Ti	W	Ni
CMSX-4	12.59	9.87	7.57	2.90	2.17	1.29	2.11	bal.
Model alloy	13.09	-	11.12	-	2.74	-	2.98	bal.
A	18.69	-	11.83	-	4.24	-	1.75	bal.
B	15.51	-	11.38	-	3.39	-	2.16	bal.

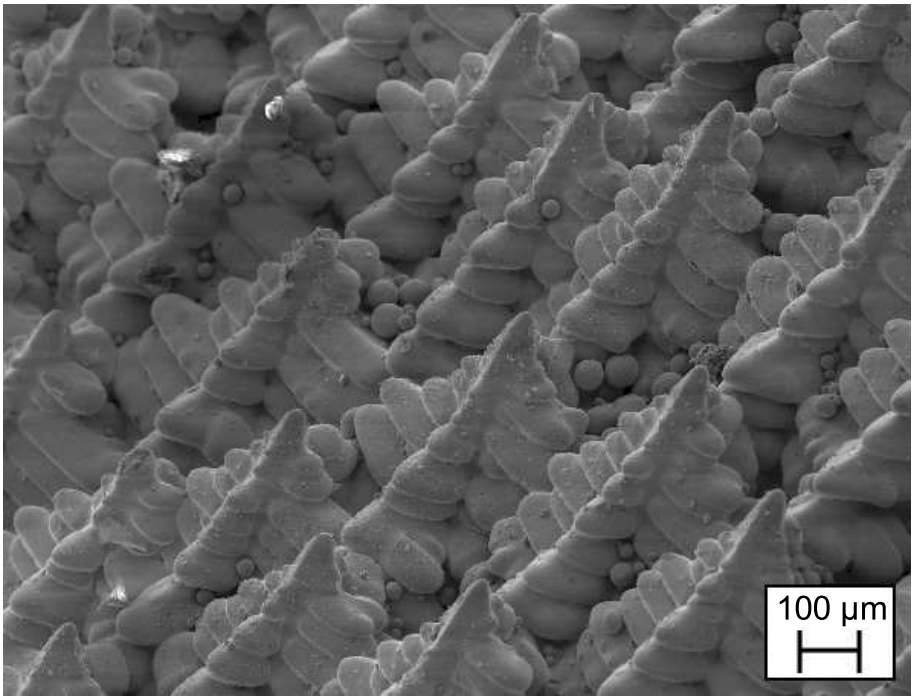

Fig. 1. The structure of the dendrites in this directionally solidified CMSX-4 sample has been revealed by an artificial bubble technique. The growing dendrites can be clearly distinguished from the sphere like interdendritic γ' phase.

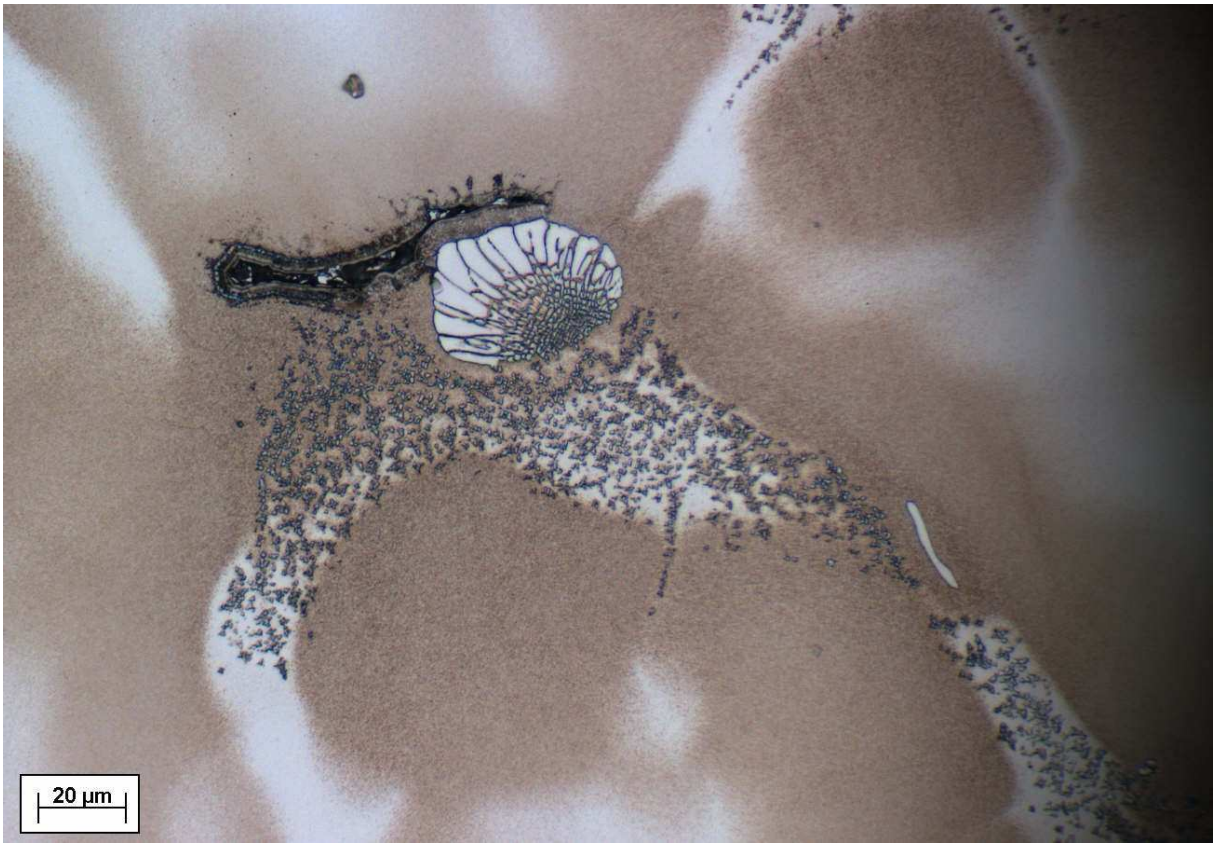

Fig. 2. Light optical micrograph of a directionally solidified sample of CMSX-4 interdendritic phases.

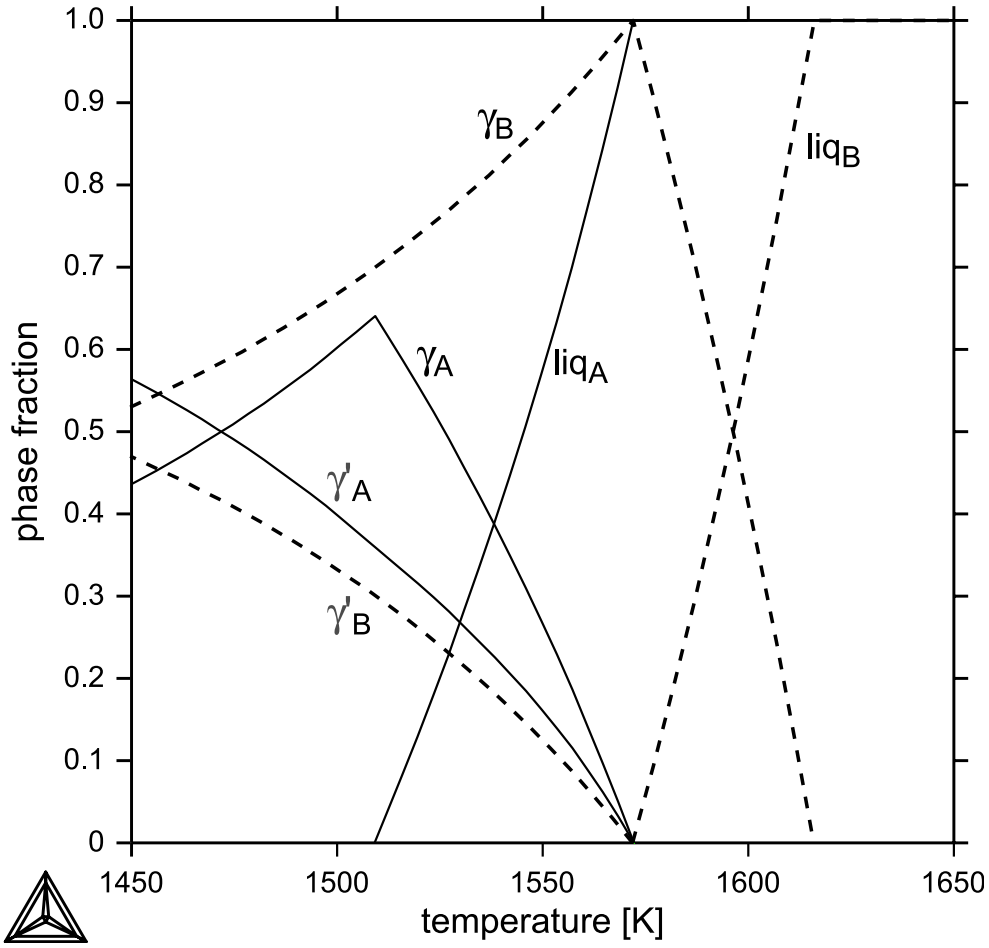

Fig. 3. Calculation of the Lever Rule transformation for the composition of the interdendritic liquid (comp A, solid lines) and the corresponding solid composition (comp B, dashed lines), as given in table 1.

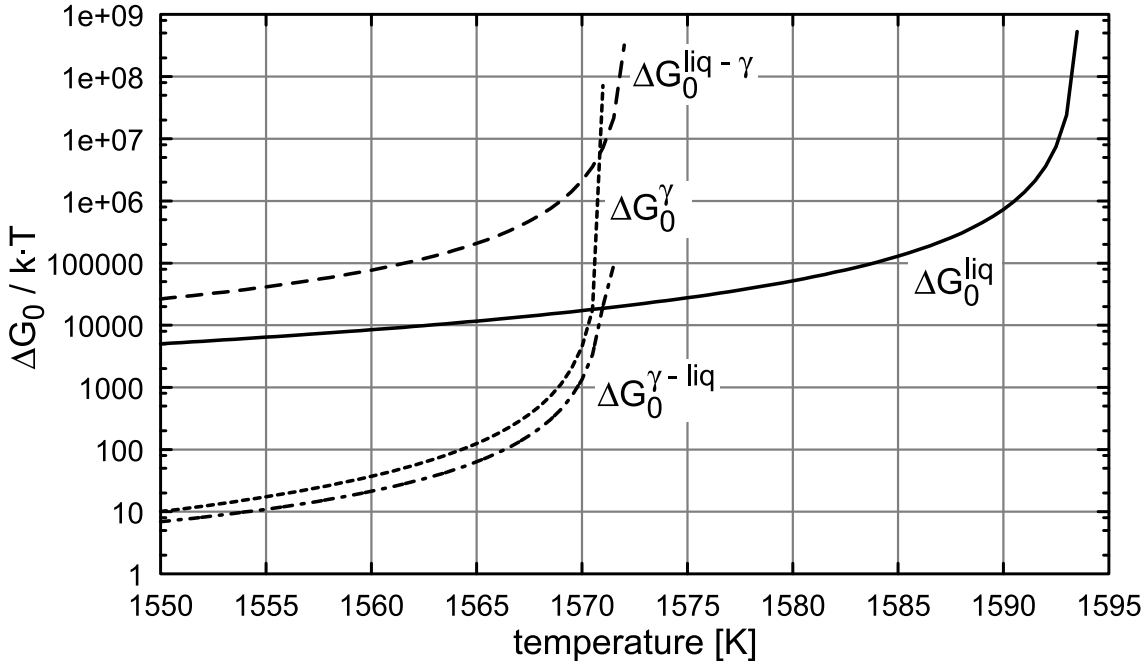

Fig. 4. Work necessary to form a γ' nucleus as a function of temperature. The superscripts indicate the corresponding nucleation sites, liq and γ for nucleation in the liq resp. γ bulk, $liq-\gamma$ and $\gamma - liq$ for nucleation at the liq resp. the γ side of the interface.

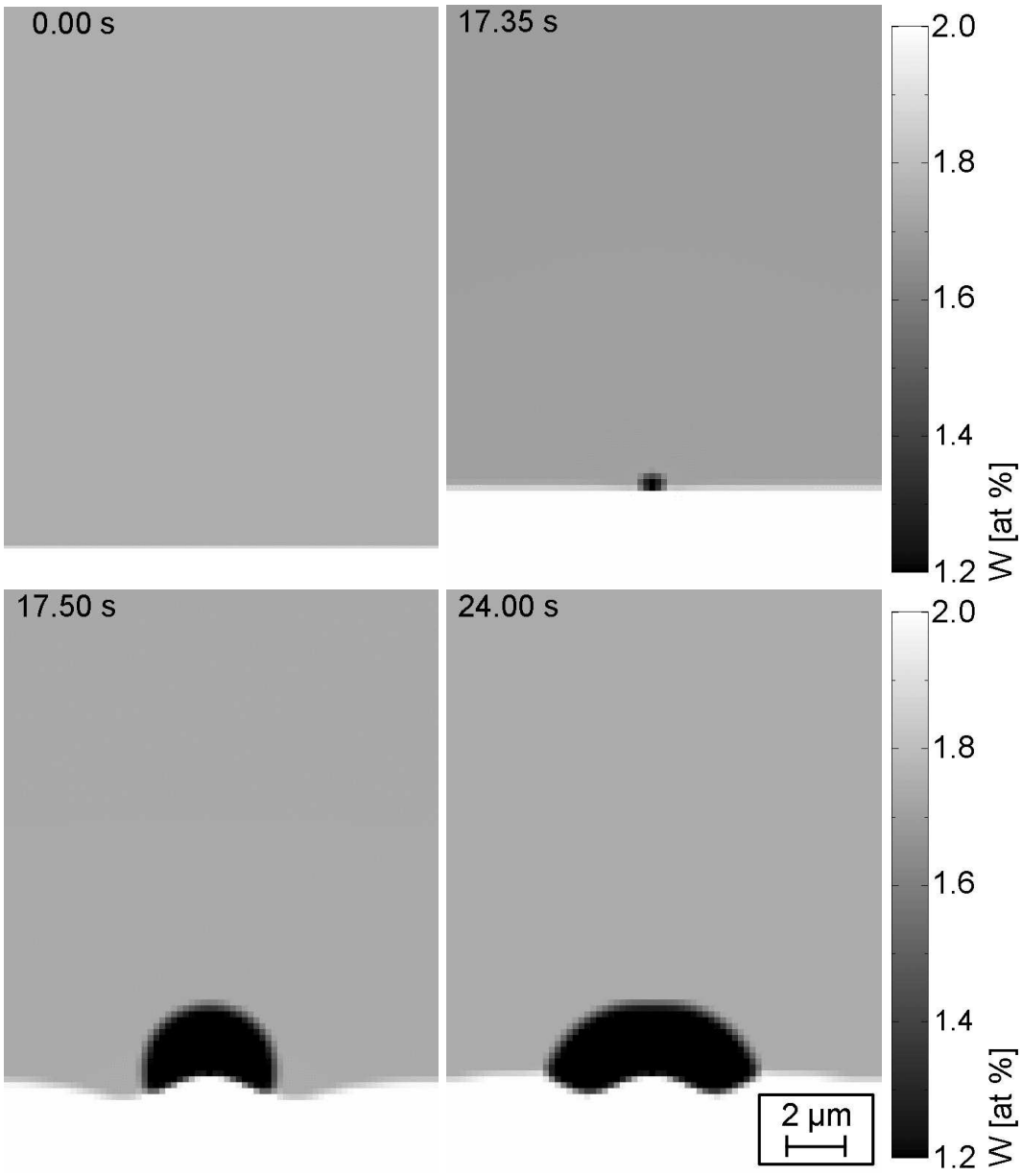

Fig. 5. Results of microstructure simulations obtained by using the phase-field method. After the nucleation rapid growth of γ' can be seen.

Fig. 1 The structure of the dendrites in this directionally solidified CMSX-4 sample has been revealed by an artificial bubble technique. The growing dendrites can be clearly distinguished from the sphere like interdendritic γ' phase.

Fig. 2 Light optical micrograph of a directionally solidified sample of CMSX-4 that shows interdendritic phases.

Fig. 3 Calculation of the Lever Rule transformation for the composition of the interdendritic liquid (comp A, solid lines) and the corresponding solid composition (comp B, dashed lines), as given in table 1.

Fig. 4 Work necessary to form a γ' nucleus as a function of temperature. The subscripts indicate the corresponding nucleation sites, liq and γ for nucleation in the liq resp. γ bulk, $liq - \gamma$ and $\gamma - liq$ for nucleation at the liq resp. the γ side of the interface.

Fig. 5 Results of microstructure simulations obtained by using the phase-field method. After the nucleation rapid growth of γ' can be seen.